



Effect of electronic excitation on high-temperature flows of ionized nitrogen and oxygen mixtures behind strong shock waves

V. A. Istomin and E. V. Kustova

Citation: [AIP Conference Proceedings](#) **1786**, 150003 (2016); doi: 10.1063/1.4967644

View online: <http://dx.doi.org/10.1063/1.4967644>

View Table of Contents: <http://scitation.aip.org/content/aip/proceeding/aipcp/1786?ver=pdfcov>

Published by the [AIP Publishing](#)

Articles you may be interested in

[Effect of electronic excitation on high-temperature flows behind strong shock waves](#)

AIP Conf. Proc. **1628**, 1221 (2014); 10.1063/1.4902731

[Transport properties of five-component nitrogen and oxygen ionized mixtures with electronic excitation](#)

AIP Conf. Proc. **1501**, 168 (2012); 10.1063/1.4769496

[Ionization behind strong normal shock waves in argon](#)

Phys. Fluids **29**, 3618 (1986); 10.1063/1.865790

[Multistep initial ionization behind strong shock waves in argon](#)

J. Chem. Phys. **61**, 1369 (1974); 10.1063/1.1682062

[Electron Temperature and Relaxation Phenomena behind Shock Waves](#)

J. Chem. Phys. **57**, 760 (1972); 10.1063/1.1678312

Effect of Electronic Excitation on High-Temperature Flows of Ionized Nitrogen and Oxygen Mixtures behind Strong Shock Waves

V. A. Istomin^{a)} and E. V. Kustova

Saint Petersburg State University, 7/9 Universitetskaya nab., St. Petersburg, 199034, Russia

^{a)}Corresponding author: vladimir_istomin@ifea.spbu.ru

Abstract. Strongly non-equilibrium flows of reacting five-component ionized mixtures of nitrogen ($N_2/N_2^+/N/N^+/e^-$) and oxygen ($O_2/O_2^+/O/O^+/e^-$) behind the plane shock wave are studied taking into account electronic degrees of freedom of both neutral and ionized species. The kinetic scheme includes non-equilibrium reactions of ionization, dissociation, recombination and charge-transfer. Two test cases corresponding to the spacecraft re-entry (Hermes and Fire II experiments) are considered; fluid-dynamic variables, transport coefficients and heat flux are calculated, and different contribution to the heat flux are analyzed. The effect of electronic excitation on the heat transfer is governed by the competition of diffusion and heat conduction; it becomes weak if diffusive processes prevail. An important role of thermal diffusion in ionized flows is emphasized. The influence of dissociation rates on the heat flux is assessed.

Introduction

Growing interest to theoretical studies of high-temperature reacting flows with excited electronic degrees of freedom is connected to problems of spacecraft (re)entry to planetary atmospheres and design of thermal protection systems. In recent works [1, 2, 3, 4, 5, 6, 7] it was shown that internal thermal conductivity coefficient associated to electronically excited states may considerably exceed that of translational modes, and the most significant contribution to the total thermal conductivity of high-temperature mixtures is given by electronically excited atomic species. Preliminary results on the heat transfer in a shock heated ionized nitrogen mixture were reported in [6]. However no systematic studies of the influence of electronic excitation on the diffusion and energy transport in real gas flows were performed.

The objective of the present study is to generalize the model proposed in [6] for the case of five-component partially ionized oxygen mixture, to calculate transport coefficients and evaluate various contributions to the heat flux in a flow behind the shock wave. We consider ($O_2/O_2^+/O/O^+/e^-$) and ($N_2/N_2^+/N/N^+/e^-$) mixtures taking into account rotational, vibrational and electronic degrees of freedom in molecules and molecular ions as well as electronically excited states in atoms and atomic ions. Dissociation, ionization and charge transfer reactions are implemented into equations of non-equilibrium chemical kinetics. Transport coefficients are calculated with the use of algorithms proposed in [3, 4]. The set of governing equations is solved numerically for the one-dimensional flow behind the shock wave under conditions of Hermes and Fire II reentry [8]. Peculiarities of heat transfer in different mixtures are discussed. Finally, the sensitivity of the heat flux to the chemical reaction rates is examined.

Governing equations and transport properties

The general set of governing equations for our problem is written in [6] for the ($N_2/N_2^+/N/N^+/e^-$) mixture; in the present study we modify the model to simulate ($O_2/O_2^+/O/O^+/e^-$) mixture flows. We consider a one-temperature chemically non-equilibrium flow assuming that translational and internal energy relaxation is fast whereas chemical reactions, ionization and transfer of charge during particles collisions proceed on the macroscopic gas-dynamic time scale. The internal energy of neutral and ionized molecules is a sum of rotational, vibrational and electronic energies; the energy of both neutral and ionized atomic species includes that of electronically excited states. The closed set

of governing equations for the macroscopic parameters taking into account electronic degrees of freedom of both molecules and atoms includes conservation equations coupled to the equations of chemical and ionization kinetics; the details of the kinetic scheme are given in the next section.

Since we focus our attention on the heat and mass transfer, let us consider diffusion velocities \mathbf{V}_c of chemical species c and heat flux \mathbf{q} . Using the procedure of the modified Chapman–Enskog method, in the viscous Navier–Stokes approximation we derive the expressions for \mathbf{V}_c and \mathbf{q} which allow one to separate contributions of different dissipative processes:

$$\mathbf{V}_c = \mathbf{V}_{c,MD} + \mathbf{V}_{c,TD}, \quad \mathbf{V}_{c,MD} = - \sum_d D_{cd} \mathbf{d}_c, \quad \mathbf{V}_{c,TD} = - D_{Tc} \nabla \ln T, \quad (1)$$

$$\mathbf{q} = \mathbf{q}_F + \mathbf{q}_{TD} + \mathbf{q}_{MD}, \quad \mathbf{q}_F = -\lambda' \nabla T, \quad \mathbf{q}_{TD} = -p \sum_c D_{Tc} \mathbf{d}_c + \sum_c \rho_c h_c \mathbf{V}_{c,TD}, \quad \mathbf{q}_{MD} = \sum_c \rho_c h_c \mathbf{V}_{c,MD}. \quad (2)$$

Here $\lambda' = \lambda_{int} + \lambda_{tr}$ is the partial thermal conductivity coefficient including contributions of the internal and translational degrees of freedom, \mathbf{d}_c is the diffusive driving force, T is the temperature, ρ_c , h_c are the density and specific enthalpy of species c ; D_{cd} , D_{Tc} are the diffusion and thermal diffusion coefficients. It is seen that the heat flux is specified by three main contributions: the Fourier flux associated to thermal conductivity \mathbf{q}_F , and fluxes due to the mass and thermal diffusion \mathbf{q}_{MD} , \mathbf{q}_{TD} .

The transport coefficients are calculated using the algorithms proposed in [3, 4]. The collision integrals are taken from [2]. In our previous papers [5, 6] we analyzed the heat conductivity of neutral and ionized species under high-temperature conditions. It was shown that for ionized atomic species, electronic excitation plays the most important role in the temperature range 25000–50000 K, where the total thermal conductivity coefficient exceeds substantially the translational one. For ionized molecular species, the influence of electronic degrees of freedom is of importance in the whole temperature range considered.

Application to a flow behind shock wave

The developed model is applied to flows of partially ionized oxygen ($O_2/O_2^+/O/O^+/e^-$) and nitrogen ($N_2/N_2^+/N/N^+/e^-$) mixtures behind a plane shock wave. Similarly to our previous simulations [6], two test cases corresponding to the specific points of re-entering spacecraft trajectories [8] are considered (TC1 and TC2). TC1 corresponds to the reentry of European space vehicle Hermes, whereas TC2 to Fire II (1634 s) experiments (see Table 1).

TABLE 1. Free-stream and post-shock conditions.

TC1: Hermes	Velocity, m/s	Temperature, K	Pressure, Pa
Pre-Shock	7198	205	2
Post-Shock	1207	24234	1763
TC2: Fire II (1634 s)	Velocity, m/s	Temperature, K	Pressure, Pa
Pre-Shock	11360	195	2
Post-Shock	1899	62377	3827

We suppose that behind the shock front, translational-rotational-vibrational as well as electronic degrees of freedom are completely excited whereas chemical reactions are frozen in the shock front; initial low-temperature mixture consists of neutral molecules. For the evaluation of the heat transfer we use the simplified post-processing algorithm (see also [9]): first, we calculate the flowfield in the Euler approximation of inviscid flow; then using the macroscopic parameters and their derivatives and applying developed transport algorithms we calculate the transport coefficients and the heat flux in a flow.

We solve numerically the following set of ordinary differential equations obtained from the general governing equations assuming that the flow is steady-state and one-dimensional:

$$\frac{d}{dx}(vn_c) = R_c, \quad c = O_2, O_2^+, O, O^+, e^-, \quad (3)$$

$$\frac{d}{dx}(p + \rho v^2) = 0, \quad (4)$$

$$\frac{d}{dx}\left(h + \frac{v^2}{2}\right) = 0, \quad (5)$$

here x is the distance from the shock front, v is the velocity, n_c is the number density of species c , p , ρ are the pressure and density, h is the specific mixture enthalpy $\rho h = \sum_c \rho_c h_c$, R_c are the production terms due to dissociation, recombination, ionization and charge-transfer processes [6]. The dissociation $k_{c,diss}^d$ and exchange $k_{c'c}^{d'd}$ reaction rate coefficients are calculated using the Arrhenius law (parameters are given in the references below). The backward reaction rate coefficients $k_{rec,c}^d$ and $k_{cc'}^{dd}$ are obtained using the detailed balance principle.

For oxygen, the following reactions are included to the kinetic scheme:

Reaction	Reference	Reaction	Reference
1. $O_2 + O_2 \rightarrow O + O + O_2$,	[10]	6. $O + O \rightarrow O_2^+ + e^-$,	[11]
2. $O_2 + O \rightarrow O + O + O$,	[10]	7. $O + O_2^+ \rightarrow O^+ + O_2$,	[11]
3. $O_2 + e^- \rightarrow O + O + e^-$,	[11]	8. $O + e^- \rightarrow O^+ + e^- + e^-$,	[11]
4. $O_2 + e^- \rightarrow O_2^+ + e^- + e^-$,	[11]	9. $O_2^+ + O_2 \rightarrow O^+ + O + O_2$.	[12]
5. $O + O \rightarrow O^+ + e^- + O$,	[13]		

The kinetic scheme used for nitrogen is given in [6]

It is worth noting that just behind the shock front, the reaction #1 starts first. All other processes have some incubation time required to accumulate active oxygen atoms and electrons; therefore the rate of this reaction may noticeably influence the rate of variation of the temperature and mixture composition in the vicinity of the shock front which, in turn, affects the heat flux. That is why we will also assess other models [14, 15] for the rate coefficient of the reaction #1.

For the above kinetic scheme the production terms have the following form:

$$R_{O_2} = R_1 + R_2 + R_3 + R_4 - R_7, \quad R_O = -2R_1 - 2R_2 - 2R_3 + R_5 + 2R_6 + R_7 + R_8 - R_9, \quad (6)$$

$$R_{O_2^+} = -R_4 - R_6 + R_7 + R_9, \quad R_{O^+} = -R_5 - R_7 - R_8 - R_9, \quad R_{e^-} = -R_4 - R_5 - R_6 - R_8. \quad (7)$$

Solving Eqs. (3)–(5) with the use of the classical fourth-order Runge-Kutta method, we find all fluid dynamic parameters (T , p , ρ , v , n_c) and their derivatives as functions of x . After that, the transport coefficients as well as the diffusion velocity (1) and heat flux (2) are evaluated.

Dynamics and heat transfer behind the shock wave

Using the approach developed above the flow parameters and the heat flux behind the shock wave in ($O_2/O_2^+/O/O^+/e^-$) and ($N_2/N_2^+/N/N^+/e^-$) mixtures under TC1 and TC2 conditions were calculated. In our simulations, we take into account the following numbers of electronic energy levels: 170 for N , 625 for N^+ and O^+ , 204 for O , 5 for N_2 , and 7 for N_2^+ , O_2 , O_2^+ , see [4, 5] for the details.

In Fig. 1 the temperature T as a function of distance x is shown for test cases Hermes (TC1) and Fire II (TC2). Behind the shock front the temperature drops fast, but the slope and final equilibrium temperature are different for oxygen and nitrogen. Due to intensive dissociation, the atomic molar fractions sharply increase up to 81% (oxygen) and 56% (nitrogen) for TC1 (Fig. 2a), and 92% (oxygen) and 79% (nitrogen) for TC2 (Fig. 2b) within the distance range $x = 0 - 1.0$ cm. For oxygen mixture, the final degree of dissociation is higher compared to nitrogen. It is surprising that for TC2 just behind the shock front nitrogen dissociates faster than oxygen and there is some delay in the temperature drop in oxygen. It can be a consequence of underestimating the rate coefficient of the reaction #1 by the McKenzie model [10]. This point will be further discussed in the end of section.

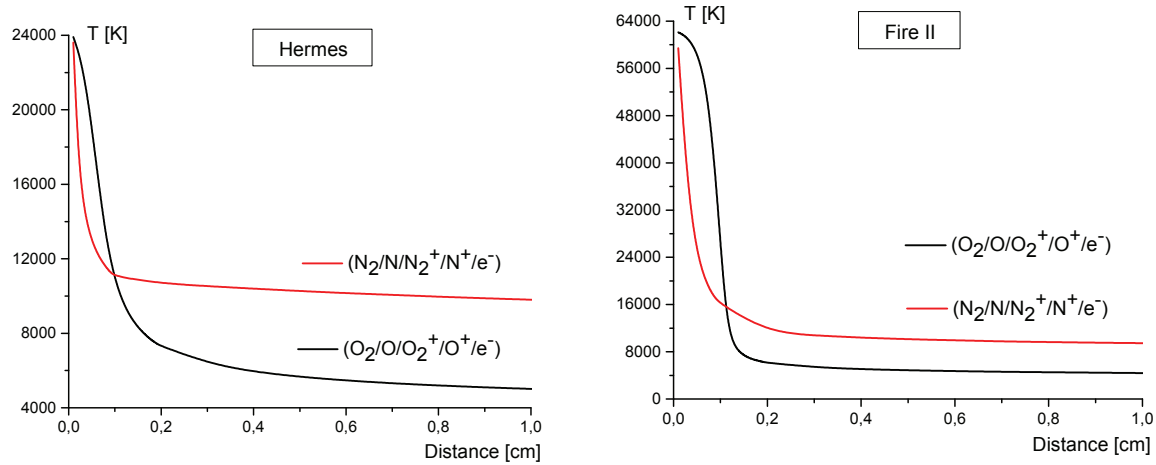


FIGURE 1. Temperature T behind the shock wave as a function of x for TC1 (Hermes) and TC2 (Fire II).

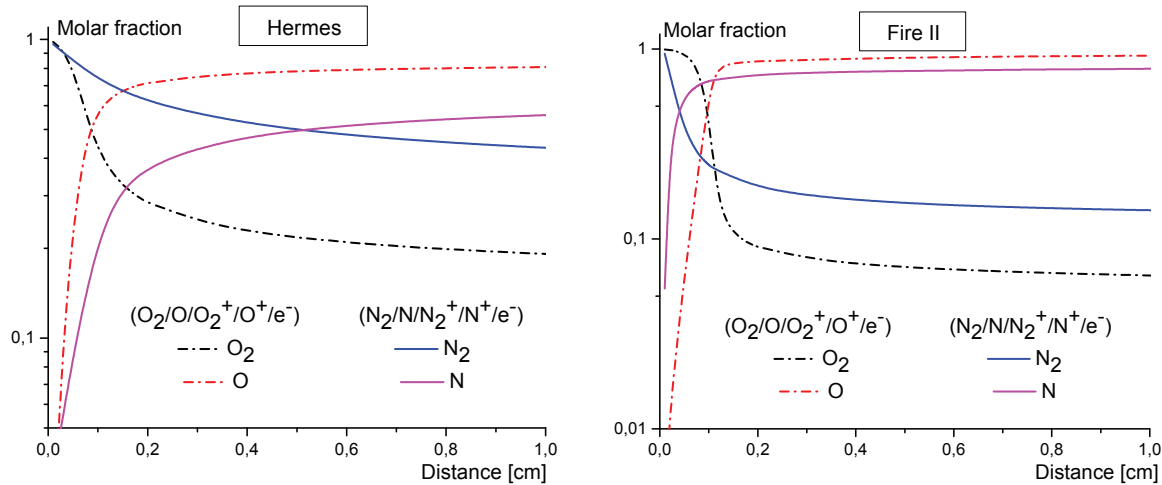


FIGURE 2. Molar fractions of neutral species behind the shock wave as functions of x for TC1 and TC2.

Under specific conditions considered in this study, the fraction of ionized species (see Fig. 3) for oxygen mixture reaches 0.01% for TC1 and 3% for TC2 within the distance range $x = 0.2 - 1.0$ cm. For nitrogen, the effect of ionization plays even greater role (0.8% (TC1) and 4% (TC2)). A decrease in molar fraction of charged particles due to recombination for $x = 0.3 - 1.0$ cm in the oxygen mixture is in line with previous investigations [16].

In Fig. 4 behavior of total thermal conductivity coefficient λ' as a function of distance x from the shock front for TC1 and TC2 is shown. Thermal conductivity coefficient was calculated taking into account electronically excited states of all species in the mixture and neglecting electronic excitation. For nitrogen mixture, the thermal conductivity coefficient in the beginning of the relaxation is about two times higher than that calculated neglecting electronic excitation for both TC1 and TC2; for oxygen mixture the influence of electronic states is lower and gives a maximum contribution about 30% (TC1) and 40% (TC2). The discrepancy decreases with x and tends to zero when temperature becomes lower than 8000 K for oxygen and 10000 K for nitrogen.

The total heat flux as well as different terms in Eq. (2) calculated taking into account and neglecting electronic excitation are presented in Figs. 5 and 6 for TC1 and in Figs. 7 and 8 for TC2. The electronic excitation influences mainly the Fourier part of the heat flux; its effect on mass diffusion is much lower and is practically negligible for thermal diffusion (we do not plot the fluxes calculated neglecting electronic excitation in Fig. 8 since the curves coincide). It is interesting that the overall effect of electronic excitation on the total heat flux strongly depends on the

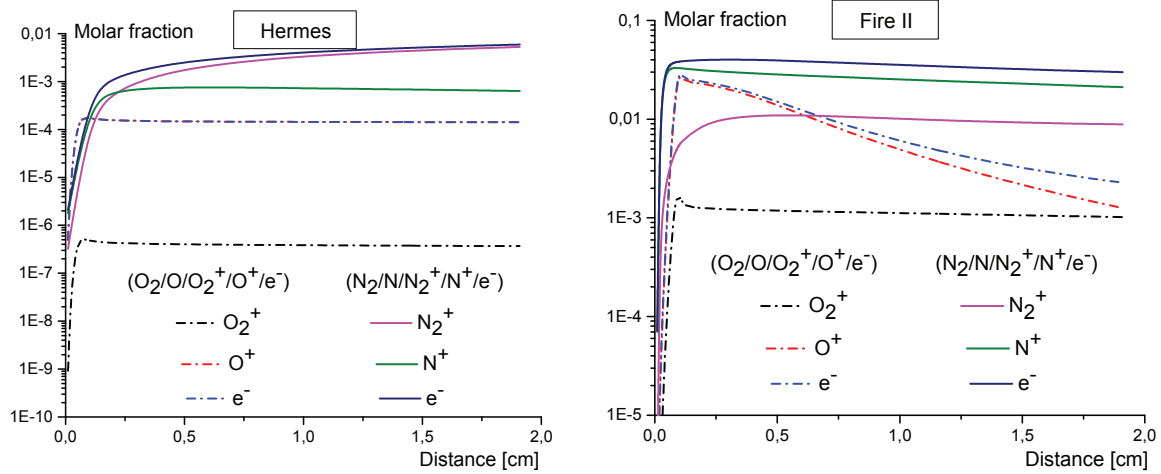


FIGURE 3. Molar fractions of charged species behind the shock wave as functions of x for TC1 and TC2.

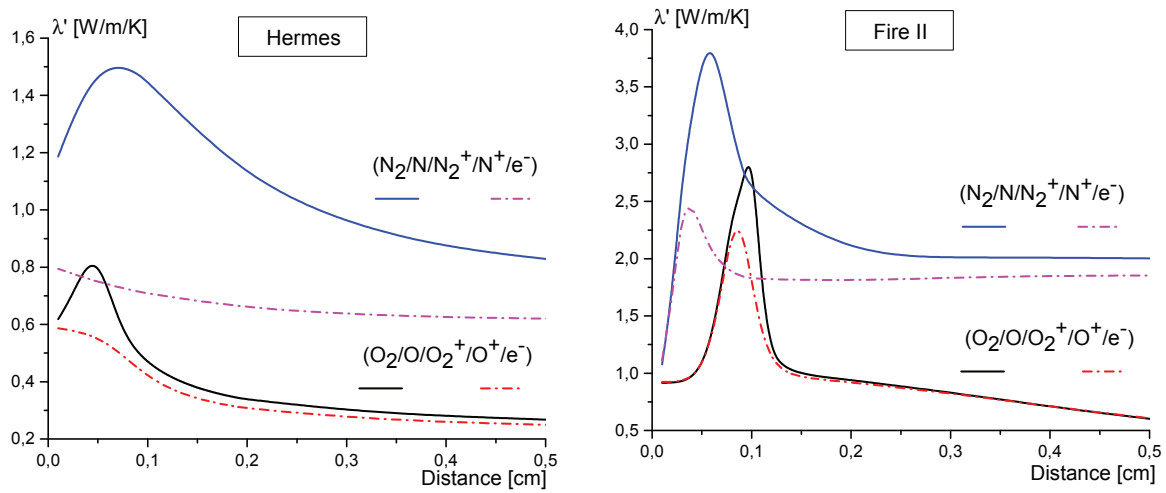


FIGURE 4. Thermal conductivity coefficient behind the shock wave as a function of distance x for TC1 and TC2 calculated taking into account electronic excitation (solid lines) and neglecting it (dash-dotted lines).

competition of different contributions to the energy transfer. Thus for TC1 all the terms in Eq. (2) are of the same order, and an important role belongs to the heat conduction, \mathbf{q}_F . This results in the considerable effect of excited electronic states on the total heat flux, especially for nitrogen (see Fig. 5a). For TC2, the main contribution to the total heat flux is given by thermal diffusion, a process which is not affected by electronic excitation; this neutralizes the strong effect of electronic energy on heat conduction and brings very weak overall effect (less than 20%) of electronic excitation on the total heat flux (see Fig. 7a).

One can notice essentially non-monotonic behavior of the heat flux and the fact that it changes its sign. It is connected, again, with the competition of diffusive and conductive fluxes. The Fourier flux behind the shock wave is always positive since the temperature decreases with x ; the mass diffusion flux is negative because of formation of new chemical species carrying higher enthalpy compared to initial molecular species; on the contrary, thermal diffusion flux alternates its sign since it depends on both temperature and molar fraction gradients. Non-monotonic behavior of the total heat flux in non-ionized mixtures behind the shock wave was emphasized also in [9] for high Mach numbers. However for neutral gases the effect of thermal diffusion is found to be negligibly weak. It is rather unusual to find such a strong effect of thermal diffusion. Nevertheless it was already reported in [6] for ionized nitrogen flows and attributed to large values of thermal diffusion coefficients for electrons. If the flow is exposed to electro-magnetic field,

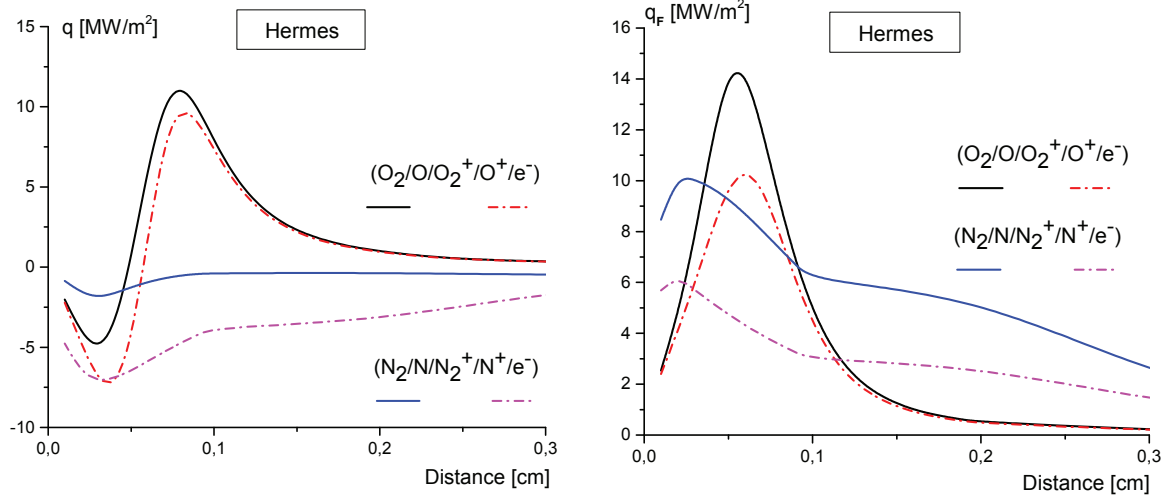


FIGURE 5. Total heat flux q and Fourier flux q_F as a function of distance x for TC1 calculated taking into account electronic excitation (solid lines) and neglecting it (dash-dotted lines).

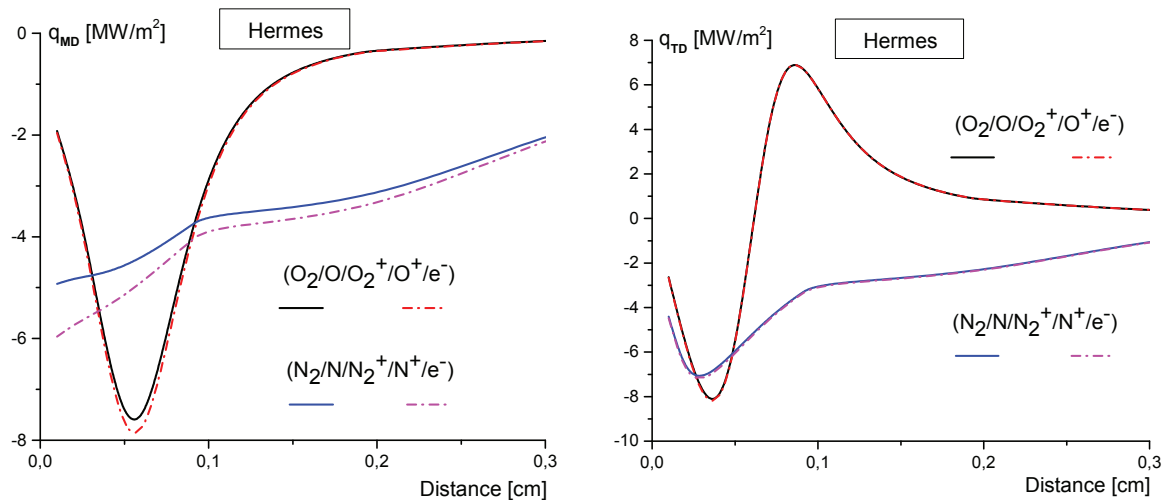


FIGURE 6. Heat fluxes due to mass diffusion q_{MD} and thermal diffusion q_{TD} as a function of distance x for TC1 calculated taking into account electronic excitation (solid lines) and neglecting it (dash-dotted lines).

the arising effect of ambipolar diffusion reduces the effect of thermal diffusion, but it is not the case in our study.

Now let us check how the model for reaction rate coefficients influences the heat transfer. As was mentioned above, using the model of McKenzie [10] for the reaction #1 yields a noticeable delay in oxygen dissociation reaction just behind the shock front which is unusual for such high-temperature flows. We implemented to our simulations the models of Park [14] and Scanlon [15] for the reaction #1. A comparison of the rate coefficients $k_1(T)$ is given in Fig. 9a; one can notice that according to the model of McKenzie k_1 decreases at high temperature. Models [14, 15] provide more reliable behavior; at high temperatures the difference is about two orders of magnitude. Applying models [14, 15] leads to faster temperature drop and higher dissociation rate in oxygen. The total heat flux calculated in oxygen for the three models is presented in Fig. 9b. It is worth noting a strong dependence of the heat flux on the reaction rates; the total flux can vary up to 1.5 times for different models; its minima and maxima are shifted towards the shock front for the models [14, 15].

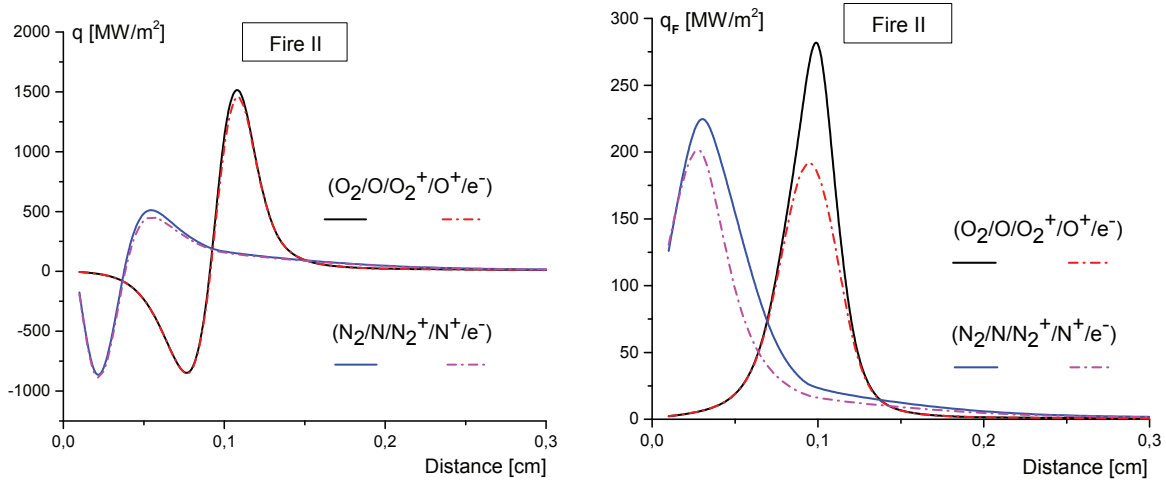


FIGURE 7. Total heat flux q and Fourier flux q_F as a function of distance x for TC2 calculated taking into account electronic excitation (solid lines) and neglecting it (dash-dotted lines).

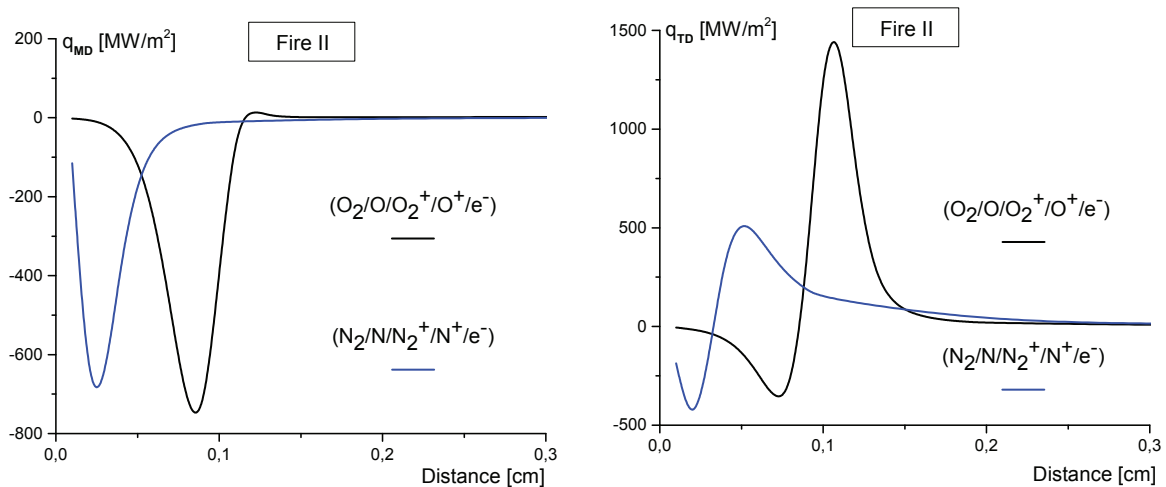


FIGURE 8. Heat fluxes due to mass diffusion q_{MD} and thermal diffusion q_{TD} as a function of distance x for TC2.

Conclusion

Strongly non-equilibrium one-dimensional steady-state flows of chemically reacting nitrogen ($N_2/N_2^+/N/N^+/e^-$) and oxygen ($O_2/O_2^+/O/O^+/e^-$) mixtures behind the plane shock wave are studied taking into account electronic degrees of freedom of both neutral and ionized species. Two test cases of Hermes and Fire II experiments are considered. Electronic degrees of freedom are of importance for the calculation of thermal conductivity coefficients close to the shock front; their contribution becomes weak for temperatures below 10000 K for nitrogen and 8000 K for oxygen. Different terms in the total heat flux are analyzed. In the beginning of the relaxation zone for the Hermes case, the contributions of thermal conductivity, mass diffusion and thermal diffusion to the total heat flux are of the same order for both mixture flows whereas for the Fire II test case, diffusion processes play dominating role in the heat transfer. Essentially non-monotonic behavior of the heat flux is explained by the competition of different dissipative processes. The heat flux depends significantly on the chemical reaction rates; it is shown that using the McKenzie model yields overpredicted heat flux and shifts its maximum away from the shock front.

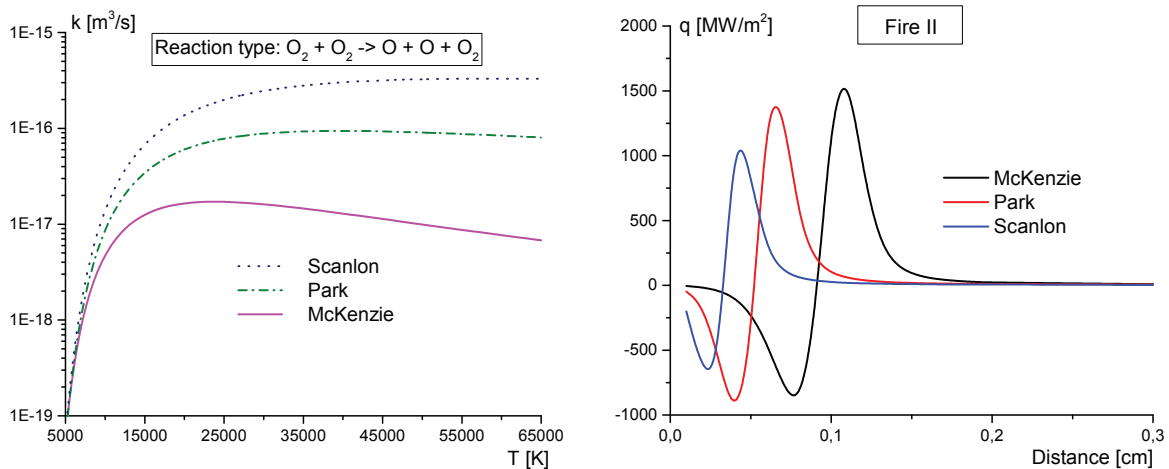


FIGURE 9. Reaction rate coefficient k_1 as a function of T and total heat fluxes q as a function of distance x for TC2 calculated using the models [10, 14, 15].

ACKNOWLEDGMENTS

The research leading to these results has received funding from the Russian Foundation for Basic Research (projects 14-01-31037 and 16-38-60009) and Saint Petersburg State University, project 6.37.163.2014. Also we are grateful to Saint Petersburg State University for the travel grant 6.41.701.2016, which made possible participation in the RGD30.

REFERENCES

- [1] D. Bruno, A. Laricchiuta, M. Capitelli, and C. Catalfamo, *Phys. Plasmas* **14**, p. 022303 (2007).
- [2] D. Bruno, M. Capitelli, C. Catalfamo, R. Celiberto et al., “Transport properties of high-temperature mars-atmosphere components,” ESA STR 256 (ESA, Noordwijk: ESA Publications Division, 2008).
- [3] E. Kustova and L. Puzyreva, *Phys. Rev. E* **80**, p. 046407 (2009).
- [4] V. Istomin, E. Kustova, and L. Puzyreva, “Transport properties of electronically excited N_2/N and O_2/O mixtures,” in *Rarefied Gas Dynamics*, AIP Conference Proceedings, Vol. 1333, edited by D. Levin et al. (American Institute of Physics, Melville, NY, 2011), pp. 667–672.
- [5] V. Istomin and E. Kustova, “Transport properties of five-component nitrogen and oxygen ionized mixtures with electronic excitation,” in *Rarefied Gas Dynamics*, AIP Conference Proceedings, Vol. 1501, edited by M. Mareschal and A. Santos (American Institute of Physics, Melville, NY, 2012), pp. 168–174.
- [6] V. Istomin and E. Kustova, “Effect of electronic excitation on high-temperature flows behind strong shock waves,” in *Rarefied Gas Dynamics*, AIP Conference Proceedings, Vol. 1628, edited by J. Fan (American Institute of Physics, Melville, NY, 2014), pp. 1221–1228.
- [7] V. A. Istomin, E. V. Kustova, and M. A. Mekhonoshina, *J. Chem. Phys.* **140**, p. 184311 (2014).
- [8] D. L. Cauchon, “Radiative heating results from fire ii flight experiment at a re-entry velocity of 11.4 km/s,” Tech. Rep. X-1402 (NASA, NASA Technical Memorandum).
- [9] O. Kunova, E. Kustova, M. Mekhonoshina, and E. Nagnibeda, *Chem. Phys.* **463**, 70–81 (2015).
- [10] R. Mc Kenzie and J. Arnold, AIAA Paper **67-322** (1967).
- [11] S. Selle and U. Riedel, AIAA Paper **2000-0211** (2000).
- [12] M. Capitelli, C. Ferreira, B. Gordiets, and A. Osipov, *Plasma Kinetics in Atmospheric Gases*, Springer series on atomic, optical and plasma physics, Vol. 31 (Springer-Verlag, Berlin, 2000).
- [13] G. G. Chernyi and S. A. Losev, *Physical and chemical processes in plasma gases. Guide (in Russian)* (Nauchny Mir, 2007).
- [14] C. Park, J. Howe, R. Howe, R. Jaffe, and G. Candler, *J. Thermophys. Heat Transfer* **8**, 9–23 (1994).
- [15] T. J. Scanlon, C. White, M. K. Borg, R. C. Palharini, E. Farbar, I. D. Boyd, J. M. Reese, and R. E. Brown, *AIAA Journal* **53**, 1670–1680 (2015).
- [16] M. Panesi, T. E. Magin, A. Bourdon, A. Bultel, and O. Chazot, *J. Thermophys. Heat Transfer* **23**, 236–248 (2009).